Advances in Applied Sciences
2022; 7(2): 21-26
http://www.sciencepublishinggroup.com/j/aas
doi: 10.11648/j.aas.20220702.11
ISSN: 2575-2065 (Print); ISSN: 2575-1514 (Online)

An Efficient Model in Calculating Anharmonic XAFS Debye-Waller Factor of Metal Crystals

Nguyen Thi Ngoc Anh, Nguyen Ngoc Thang, Dang Van Trong*

Faculty of Fundamental Sciences and Foreign Languages, University of Fire Prevention and Fighting, Hanoi, Vietnam

Email address:
trongdv@daihocpccc.edu.vn (D. V. Trong)

*Corresponding author

To cite this article:
Nguyen Thi Ngoc Anh, Nguyen Ngoc Thang, Dang Van Trong. An Efficient Model in Calculating Anharmonic XAFS Debye-Waller Factor of Metal Crystals. *Advances in Applied Sciences*. Vol. 7, No. 2, 2022, pp. 21-26. doi: 10.11648/j.aas.20220702.11

Received: May 25, 2022; **Accepted**: June 9, 2022; **Published**: June 20, 2022

Abstract: The X-ray absorption fine structure (XAFS) is often used effectively to determine many structural parameters and dynamic properties of materials, so calculating the temperature-dependent XAFS Debye-Waller (DW) factor of metal crystals will be a necessary addition to the advanced material technique. In this work, the thermodynamic parameters are derived from the influence of the absorbing and backscattering atoms of all their nearest neighbors in the crystal lattice with thermal vibrations. The anharmonic XAFS DW factor of metal crystals has been obtained in explicit forms using the anharmonic correlated Debye (ACD) model. This calculation model is developed from the correlated Debye model using the anharmonic-effective potential and many-body perturbation approach. The numerical results for the crystalline cadmium are in good agreement with those obtained by the other theoretical model and experimental data at several temperatures. The analytical results show that the ACD model is useful and efficient in calculating the anharmonic XAFS DW factor of metal crystals. This model can be applied to calculate the anharmonic XAFS DW factor for other metals from above absolute zero temperature to just before the melting point.

Keywords: Anharmonic XAFS Debye-Waller Factor, Metal Crystals, Anharmonic Correlated Debye Model

1. Introduction

In recent years, the X-ray absorption fine structure (XAFS) is widely used to determine many dynamic properties and structural parameters of materials [1-4], and it has been developed into a powerful technique. However, the position of atoms is not stationary, and their interatomic always changes due to thermal vibrations [5, 6]. These thermal vibrations are sensitive to XAFS oscillation, so they cause the anharmonic effects and thermal disorders on crystal vibrations and will smear out the XAFS oscillations [6, 7]. In order to analyze the anharmonic XAFS signals caused by these thermal disorders, Bunker proposed a cumulant expansion approach to represent the anharmonic XAFS oscillation via the moments of the radial distribution (RD) function [8, 9]. In this approach, the anharmonic XAFS oscillation function is often written by means of XAFS cumulants that contain the second XAFS cumulant $\sigma^2(T)$ corresponding to the parallel mean-square relative displacement (MSRD) and describing anharmonic XAFS Debye-Waller (DW) factor [8, 10]. This factor is sensitive to short-range correlations of atomic fluctuations and can be used to examine the anharmonicity effects [11, 12]. It is an important factor in anharmonic XAFS analysis because it can characterize the anharmonic XAFS thermodynamic properties and describe the anharmonic XAFS amplitude reduction [13, 14].

Nowadays, metals and advances in manufacturing processes have brought us the industrial revolutions, so it becomes irreplaceable materials in the growth of human civilization. They are used extensively in manufacturing machines for automobiles, farming or agriculture, and industries, including rockets, airplanes, railways, road vehicles, etc. [15-18]. The XAFS DW factor of metal crystals has also been investigated using the general anharmonic correlated Einstein (GACE) [19] and the classical anharmonic correlated Einstein (CACE) [20] models and experiments [19, 20]. Still, this model only uses a unique correlated Einstein frequency to describe the atomic vibrations, so it

cannot mimic the acoustic phonon branches presencing in lattice crystals.

Recently, an anharmonic correlated Debye (ACD) model [21] can treat even the acoustic phonons branches presencing in lattice crystals. It has also been efficiently used to investigate the anharmonic XAFS cumulants of many materials [22-24]. Still, it has not yet been used to analyze the anharmonic XAFS DW factor of metal crystals. Therefore, calculating the temperature-dependent XAFS DW factor of metal crystals based on extending the ACD model will be a necessary addition to experimental data analysis in the advanced material technique.

2. Basic Formulae of XAFS DW Factor

The *K*-edge EXAFS function in the framework of plane-wave approximation for one scattering path, including a non-Gaussian disorder, can be expressed via a canonical average by [8-11]

$$\chi(k)=\frac{NS_0^2(k)}{k}F(k)Im\left\{\left\langle\frac{e^{-2r/\lambda}}{r^2}\mathrm{e}^{2ikr}\right\rangle e^{i\delta(k)}\right\}, \quad (1)$$

where r depends on the temperature T and is the instantaneous distance between the backscattering and absorbing atoms, λ is the electron mean free path, the angular bracket $\langle\ \rangle$ is the thermal average, $\delta(k)$ is the net phase shift, N is the coordination number, $S_0^2(k)$ is the square of the many-body overlap term, $F(k)$ is the atomic backscattering amplitude, and k is the photoelectron wavenumber.

Usually, the analysis of the temperature-dependent XAFS spectra using the XAFS cumulants expressed in terms of the power moments of the RD function [8, 9], so the second XAFS cumulant can be given by [25, 26]

$$\sigma^2(T)=\left\langle\left(r-\langle r\rangle\right)^2\right\rangle=\left\langle x^2\right\rangle-\langle x\rangle^2,\ x=r-r_0, \quad (2)$$

where r_0 is the balance distance between the backscattering and absorbing atoms and x is the deviation distance between these atoms.

In the anharmonic XAFS theory, the XAFS DW factor is usually defined via an exponential function of the second XAFS cumulant as follows [27, 28]:

$$\mathrm{W}(T,k)=\exp\left\{-2k^2\sigma^2(T)\right\}, \quad (3)$$

To determine the thermodynamic parameters of a system, it is necessary to specify the force constants and anharmonic effective (AE) potential of this system [19, 25]. In the relative vibrations of absorbing (1) and backscattering (2) atoms, taking into account only the nearest-neighbor interactions and including the effect of correlation, the AE potential [29, 30] is given using the pair interaction (PI) potential in the form:

$$V_{eff}=\varphi(x)+\sum_{i=1,2}\sum_{j\neq1,2}\varphi\left(\varepsilon_i\hat{R}_{12}\hat{R}_{ij}x\right),\ \varepsilon_i=\frac{\mu}{M_i}, \quad (4)$$

where with masses M_1 and M_2, respectively, M_i is the mass of the ith atom, the sum i is the over absorber ($i=1$) and backscatter ($i=2$), the sum j is over the nearest neighbors, $\mu=M_1M_2/(M_1+M_2)$ is the reduced mass of the absorber and backscatter, $\hat{R}$ is a unit vector, x is the deviation distance between the absorber and backscatter, D is the dissociation energy, α is the width of the potential, and $\varphi(x)$ is the PI potential of the metals and is usually determined [31, 32] from the Morse potential as

$$\varphi(x)=D\left(\mathrm{e}^{-2\alpha x}-2e^{-\alpha x}\right), \quad (5)$$

For the monatomic crystals, all atoms have M_i equals m, so ε_i equals ½. Calculating the AE potential of this monatomic system from Eqs. (4)-(5) and ignoring the constant contribution, the result is obtained in the expressed form up to the fourth-order as

$$V_{eff}\simeq\frac{1}{2}k_{eff}x^2-k_3x^3+k_4x^4, \quad (6)$$

where k_{eff} is the effective force constant, k_3 is the local force constant giving asymmetry of potential due to the inclusion of anharmonicity, and these force constants are considered in the temperature-independent [25, 26].

The general expression of the second EXAFS cumulants in the ACD model was calculated in the temperature dependence by Hung *et al.* [21]. Still, these obtained expressions are not optimized yet because they still depend on the lattice constant a. In this investigation, the previous ACD model has been extended to calculate the temperature-dependent XAFS DW factor of metal crystals.

The ACD model is perfected based on the correlated Debye model [33] using the AE potential [29] and many-body perturbation approach [21] and is derived from the dualism of an elementary particle in quantum theory [34]. In this model, a system consisting of many phonons can treat and quantize the atomic vibrations, in which a wave having a frequency $\omega(q)$ corresponds to each atomic vibration and is described via the dispersion relation [22-24]:

$$\omega(q)=\omega_D\left|\sin\left(\frac{qa}{2}\right)\right|,\ \omega_D=2\sqrt{\frac{k_{eff}}{m}}=\sqrt{2}\omega_E,\ |q|\le\frac{\pi}{a}, \quad (7)$$

where q is the phonon wavenumber in the first Brillouin (FB) zone, a is the lattice constant, ω_E is the correlated Einstein frequency, and ω_D is the correlated Debye frequency and characterizes the atomic thermal vibrations.

After using the general expression of the second EXAFS cumulants and converting from variable q to variable p in the formula $p=qa/2$, the temperature-dependent second XAFS cumulants of metal crystals are obtained in the form as

$$\sigma^2(T)=\frac{\hbar}{\pi k_{eff}}\int_0^{\pi/2}\omega(p)\frac{1+\exp\{-\hbar\omega(p)/k_BT\}}{1-\exp\{-\hbar\omega(p)/k_BT\}}dp$$
$$=\frac{\hbar}{\pi k_{eff}}\int_0^{\pi/2}\omega(p)\coth\{\hbar\omega(p)/2k_BT\}dp \quad (8)$$

Substituting this expression into the Eq. (3) to calculate the temperature-dependent XAFS DW factor of metal crystals, which obtains the following result:

$$W(T,k)=\exp\left\{-\frac{2\hbar k^2}{\pi k_{eff}}\int_0^{\pi/2}\omega(p)\coth\{\hbar\omega(p)/2k_BT\}dp\right\}, \quad (9)$$

Using an approximation $\exp\{-\hbar\omega(p)/k_BT\}\approx 0$, the temperature-dependent XAFS DW factor of metal crystals at the high-temperature (LT) limit ($T\to 0$) can be calculated from Eq. (9), and the obtained result is

$$W(T,k)\simeq\exp\left\{-\frac{2\hbar k^2\omega_D}{\pi k_{eff}}\right\}, \quad (10)$$

Using an approximation $\exp\{-\hbar\omega(p)/k_BT\}\approx 1-\hbar\omega(p)/k_BT$, the temperature-dependent XAFS DW factor of metal crystals in the high-temperature (HT) limit ($T\to\infty$) can be calculated from Eq. (9), and the obtained result is

$$W(T,k)\simeq\exp\left\{-\frac{2k^2k_BT}{k_{eff}}\right\}, \quad (11)$$

Thus, an extended ACD model has been perfected to efficiently calculate the temperature dependence of the TE coefficient of metal crystals. The obtained expressions using this model can satisfy all their fundamental properties in the temperature-dependent. These expressions have also been optimized to not depend on the lattice constant a as in the previous ACD model [21, 23].

3. Results and Discussions

To discuss the efficiency of the present theoretical model in calculating the anharmonic XAFS DW factor of metals, the obtained expressions using the ACD model from Sec. 2 are used to calculate the numerical results for crystalline cadmium (Cd). This metal has a hexagonal close-packed (HCP) structure [16], as seen in Figure 1. For monatomic crystals like Cd, each atom is similar in mass $m_i = m$ and is bonded to twelve other surrounding atoms in the first shell [35].

In these numerical calculations, the atomic mass $m = 112.410$ u [36], Morse potential parameters $\alpha = 1.907$ Å^{-1}, $D = 0.168$ eV, and $r_0 = 3.042$ Å [19], and the lattice constants a = 2.98 Å, c = 5.62 Å, and e = 1.89 [36] are used to calculate the local force constants, the AE potential, the correlated Debye frequency, and the anharmonic second EXAFS cumulant and XAFS DW factor. The following is the presentation of these numerical results:

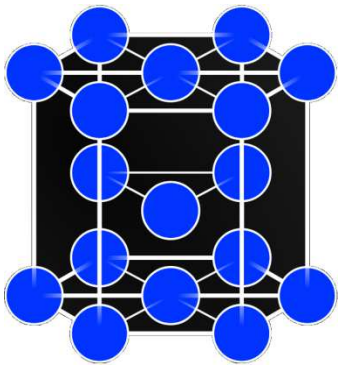

Figure 1. *The crystal model of Cd with an HCP structure.*

Using Eqs. (4)-(7) in the ACD model, it obtains the local force constants $k_{eff} \simeq 2.975$ eVÅ^{-2}, $k_3 \simeq 1.429$ eVÅ^{-3}, and $k_4 \simeq 1.521$ eVÅ^{-4} and the correlated Debye frequency $\omega_D \simeq 3.186\times10^{13}$ Hz. It can be seen that these obtained values fit well with those obtained using the GACE [19] and CACE [20] models and experimental data [19] in the previous works.

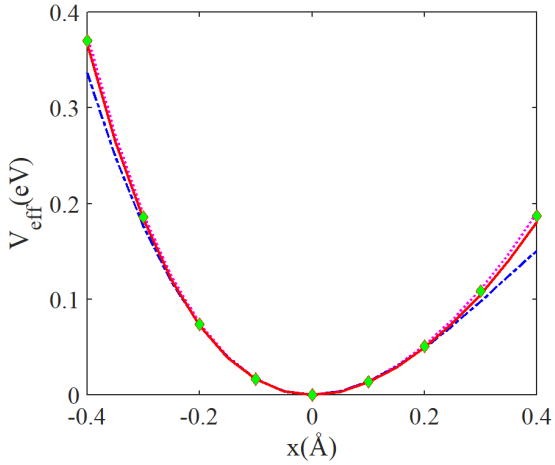

Figure 2. *The position-dependent AE potential of Cd obtained from the ACD (solid red line), GACE [19] (dashed-dotted green line), and CACE [20] (dotted magenta line) models and experimental data [20] (full green diamonds).*

The position dependence of the AE potential of Cd is calculated from Eq. (6) in the position range from -0.4 to 0.4 Å and is represented in Figure 3. Herein, the obtained result in this work is calculated from the above force constants, and those obtained using experimental data are derived from the measured Morse potential parameters $\alpha = 1.905$ Å^{-1}, $D = 0.165$ eV, and $r_0 = 3.055$ Å [19]. Meanwhile, the obtained result using the GACE model [19] does not take into account the anharmonic force constant k_4 in this equation, and those obtained using the CACE model [20] does not consider the structural distortion of Cd in this calculation. It can be seen that the obtained results using the ACD model fit with those obtained using the ACE [19] and

CACE [20] models and experimental data [19]. Moreover, in comparison with the obtained result using the experimental data [19], the obtained results using the ACD model fit better than those obtained using other models [19, 20], as seen in Figure 2.

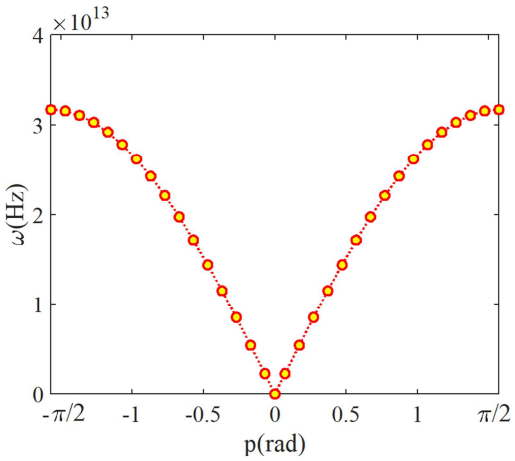

Figure 3. *The wavenumber-dependent frequency of Cd within the ACD model.*

The wavenumber dependence of the frequency of Cd in the FB zone is calculated from Eq. (7) and is represented in Figure 3. It can be shown that the obtained frequency using the ACD is a symmetric function of a linear chain of p, and its maximum value is ω_D at the bounds of the FB zone with $p = \pm\pi/2$. This result is similar to the result calculated for other crystals in the previous work [22, 24].

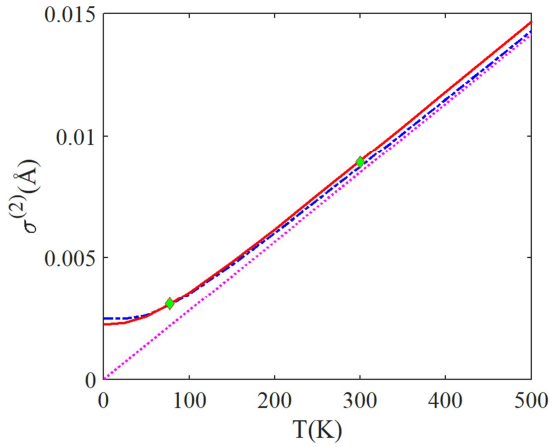

Figure 4. *Temperature-dependent second EXAFS cumulant of Cd obtained using the ACD (solid red line), CACE [20] (dotted magenta line), and GACE [19] (dashed-dotted green line) models and experiment [20] (full green diamonds).*

The second XAFS cumulant $\sigma^2(T)$ of Cd in the temperature-dependence is shown in Figure 4. Herein, the obtained result in this work is calculated from Eq. (8), and the experimental values at 77 K and 300 K [19] are derived from measured EXAFS data analysis. It can be seen that the obtained result using the ACD model agrees well with those obtained from the GACE [19] and CACE (only in the high-temperature region) [20] models and experiment [19], in which the obtained result in this work is in best agreement with the experimental values. For example, the obtained results using the ACD model, GACE model [19], and CACE model [20], and experimental data [19] at T = 77 K are $\sigma^2 \simeq 3.07\times10^{-3}$ Å^2, $\sigma^2 \simeq 3.04\times10^{-3}$ Å^2, $\sigma^2 \simeq 2.18\times10^{-3}$ Å^2, and $\sigma^2 \simeq 3.10\times10^{-3}$ Å^2, respectively, while the corresponding results at T = 300 K are $\sigma^2 \simeq 8.96\times10^{-3}$ Å^2, $\sigma^2 \simeq 8.73\times10^{-3}$ Å^2, $\sigma^2 \simeq 8.49\times10^{-3}$ Å^2, and $\sigma^2 \simeq 8.91\times10^{-3}$ Å^2, respectively. Also, in the LT region, the obtained result using the GACE model [19] is slightly greater than the obtained result using the ACD model because the ACE model use only one effective frequency to describe the atomic thermal vibrations. Meanwhile, the CACE model [20] approaches zero as the temperature approaches the zero-point (ZP) because it cannot calculate the ZP energy and quantum effects using classical statistical theory, as seen in Figure 4.

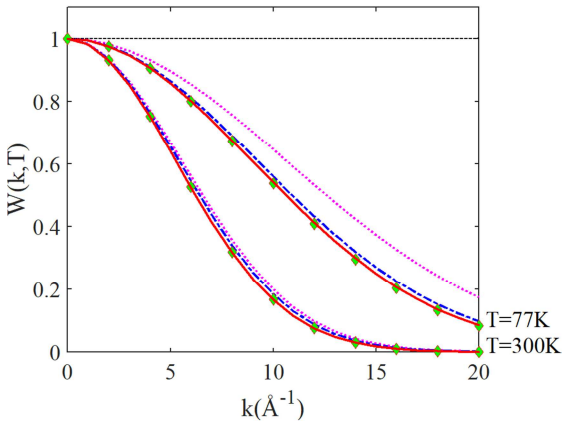

Figure 5. *Influence of temperature change on wavenumber-dependent XAFS DW factor of Cd obtained using the ACD (solid red lines), CACE [20] (dotted magenta lines), and GACE [19] (dashed-dotted green lines) models and experimental XAFS cumulant [20] (full green diamonds).*

The wavenumber dependence of the XAFS DW factor of Cd at 77 K and 300 K and in a range from 0 to 20 Å is represented in Figure 5. The obtained results are calculated from Eq. (9) with the temperature-dependent XAFS cumulant obtained using the ACD, GACE [19], and CACE [20] models and experiments. It can be seen that the obtained results using the ACD model have a reasonable characterization with those obtained using the GACE [19] and CACE [20] models and fit best with those obtained using experimental XAFS cumulant [19] in comparison with other models. Also, the small difference in the obtained results using the GACE [19] is because this model does not account for the effect of structural distortion on the second XAFS cumulant. Meanwhile, the nonconformity of obtained results using the CACE model at 77 K [20] is because this model does not work well in the LT region. For example, the obtained results using the ACD model, GACE model [19], CACE model [20], and experimental XAFS cumulant [19] at T = 77 K with k = 10 Å^{-1} and 20 Å^{-1} are W ≃ 0.5412 and 0.0858, W ≃ 0.5599 and 0.0983, W ≃ 0.6466 and 0.1748, and W ≃ 0.5379 and 0.0837, respectively, while the corresponding results at T = 300 K are W ≃ 0.1667 and 0.0007, W ≃ 0.1853 and 0.0012, W ≃ 0.2007 and 0.0016,

and $W \simeq 0.1683$ and 0.008, respectively. Moreover, It can be seen that the values of the XAFS DW factor decrease with fast-increasing wavenumber k and decrease with increasing temperature T. It is because the XAFS DW factor is an inverse function of the wavenumber k and second XAFS cumulant $\sigma^{(2)}(T)$, in which this cumulant increases with increasing temperature T, as seen in Eq. (3) and Figure 5.

4. Conclusions

In this investigation, an efficient model has been expanded to calculate the anharmonic XAFS DW factor of metals. The calculated result of the XAFS DW factor using the present ACD model decreases with increasing temperature T and satisfies all of their fundamental properties. It means that the XAFS amplitude decreases more strongly at higher temperatures. This result can also describe the influence of the anharmonic effects at high temperatures and quantum effects at low temperatures on the XAFS DW factor.

The good agreement of the numerical results of Cd in this work with those obtained using the GACE model and CACE models and experimental data at various temperatures shows the effectiveness of the present model in investigating the anharmonic XAFS DW factor. This model can be applied to calculate the anharmonic XAFS DW factor for other metals from above absolute zero temperature to just before the melting point.

Conflicts of Interest Statement

All the authors do not have any possible conflicts of interest.

Acknowledgements

The authors would like to thank Dr. Tong Sy Tien (Duy Tan University, Danang, Vietnam) for their helpful comments on the anharmonic XAFS DW factor. This work was supported by the University of Fire Prevention and Fighting, Hanoi, Vietnam.

References

[1] P. Fornasini, R. Grisenti, M. Dapiaggi, G. Agostini, and T. Miyanaga, Journal of Chemical Physics 147, 044503 (2017).

[2] F. D. Vila, J. W. Spencer, J. J. Kas, J. J. Rehr, and F. Bridges, Frontiers in Chemistry 6, 356 (2018).

[3] T. Yokoyama and S. Chaveanghong, Physical Review Materials 3, 033607 (2019).

[4] J. J. Rehr, F. D. Vila, J. J. Kas, N. Y. Hirshberg, K. Kowalski, and B. Peng, Journal of Chemical Physics 152, 174113 (2020).

[5] E. A. Stern, B. A. Bunker, and S. M. Heald, Physical Review B 21, 5521 (1980).

[6] P. A. Lee, P. H. Citrin, P. Eisenberger, and B. M. Kincaid, Reviews of Modern Physics 53, 769 (1981).

[7] P. Eisenberger and G. S. Brown, Solid State Communications 29, 481 (1979).

[8] G. Bunker, Instruments and Methods in Physics Research 207, 437 (1983).

[9] L. Tröger, T. Yokoyama, D. Arvanitis, T. Lederer, M. Tischer, and K. Baberschke, Physical Review B 49, 888 (1994).

[10] J. M. Tranquada and R. Ingalls, Physical Review B 28, 3520 (1983).

[11] J. J. Rehr and R. C. Albers, Reviews of Modern Physics, 72, 621 (2000).

[12] Nguyen Ba Duc, Vu Quang Tho, Tong Sy Tien, Doan Quoc Khoa, and Ho Khac Hieu, Radiation Physics and Chemistry 149, 61 (2018).

[13] F. W. Lytle, D. E. Sayers, and E. A. Stern, Physical Review B 11, 4825 (1975).

[14] R. B. Greegor and F. W. Lytle, Physical Review B 20, 4902 (1979).

[15] G. Laplanche, P. Gadaud, O. Horst, F. Otto, G. Eggeler, and E. P. George, Journal of Alloys and Compounds 623, 348 (2015).

[16] A. M. Kadim, Applications of Cadmium Telluride (CdTe) in Nanotechnology, IntechOpen, London, 2019.

[17] M. Hou, L. Li, and M. Zhuang, IOP Conference Series: Earth and Environmental Science 227, 052046 (2019).

[18] N. E. Galushkin, N. N. Yazvinskaya, and D. N. Galushkin, Journal of Energy Storage 39, 102597 (2021).

[19] N. V. Hung, L. H. Hung, T. S. Tien, and R. R. Frahm, International Journal of Modern Physics B 22, 5155 (2008).

[20] N. V. Hung, T. S. Tien, N. B. Duc, and D. Q. Vuong, Modern Physics Letters B 28, 1450174 (2014).

[21] N. V. Hung, N. B. Trung, and B. Kirchner, Physica B: Condensed Matter 405, 2519 (2010).

[22] T. S. Tien, Journal of Synchrotron Radiation 28, 1544 (2021).

[23] N. V. Hung, T. T. Hue, H. D. Khoa, and D. Q. Vuong, Physica B: Condensed Matter 503, 174 (2016).

[24] T. S. Tien, European Physical Journal Plus 136, 539 (2021).

[25] T. Yokoyama, K. Kobayashi, T. Ohta, and A. Ugawa, Physical Review B 53, 6111 (1996).

[26] T. Fujikawa and T. Miyanaga, Journal of the Physical Society of Japan 62, 4108 (1993).

[27] E. D. Crozier, J. J. Rehr, and R. Ingalls, X-ray Absorption: Principles, Applications, Techniques of EXAFS, SEXAFS and XANES, edited by D. C. Koningsberger and R. Prins, Wiley, New York, 1988, Chap. 9.

[28] N. V. Hung, C. S. Thang, N. B. Duc, D. Q. Vuong, and T. S. Tien, Physica B: Condensed Matter 521, 198 (2017).

[29] N. V. Hung and J. J. Rehr, Physical Review B 56, 43 (1997).

[30] T. S. Tien, Journal of Physics D: Applied Physics 53, 315303, (2020).

[31] P. M. Morse, Physical Review 34, 57 (1929).

[32] L. A. Girifalco and V. G. Weizer, Physical Review 114, 687 (1959).

[33] G. Beni and P. M. Platzman, Physical Review B 14, 1514 (1976).

[34] G. D. Mahan, Many-Particle Physics, 2nd edition, Plenum, New York, 1990.

[35] G. Buxbaum and G. Pfaff, Industrial Inorganic Pigments, 3rd edition, Wiley-VCH, New York, 2005.

[36] P. Enghag, Encyclopedia of the elements: Technical data, history, processing, applications, Wiley-VCH, Weinheim, 2004.